

Electroactive Composite Dendrimer Films Containing Thiophene-Terminated Poly(amidoamine) Dendrimers Cross-Linked by Poly(3-methylthiophene)

Julio Alvarez, Li Sun, and Richard M. Crooks*

Department of Chemistry, Texas A&M University, P.O. Box 30012,
College Station, Texas 77842-3012

Received May 30, 2002

The preparation and characterization of electroactive, dendrimer-containing films is discussed. Polymer films were prepared by electropolymerization of a thiophene-functionalized poly(amidoamine) dendrimer (G4Th) and by electrocopolymerization of G4Th and poly(3-methylthiophene) (P3MeTh). The composite P3MeTh/G4Th film was found to consist of up to 80% of the dendrimer. Control experiments indicated that dendrimers not functionalized on their periphery with thiophene groups are not incorporated into the P3MeTh matrix. The conductivity of the composite films was the same as that of the P3MeTh-only films, although UV-vis spectroscopy indicated reduced conjugation in the composite. The dendrimer-containing films were found to sorb Pt^{2+} ions.

Introduction

In this paper, we report the synthesis of an electrochemically addressable composite thin film consisting of poly(3-methylthiophene) (P3MeTh) and poly(amidoamine) (PAMAM) dendrimers functionalized on their periphery with thiophene monomers (Scheme 1). The dendrimers in these films have a strong affinity for metal ions, and therefore, they represent a first step toward the development of dendrimer-based battery materials and electrocatalytic polymers.¹ Here we report the synthesis of these composite materials and provide information about their electrochemical and spectroscopic properties.

We^{2–10} and others^{11–17} have previously shown that it is possible to prepare monolayers of dendrimer on surfaces and that these materials have applications as adhesion promoters,^{2–4,6,7,10–12,14,15} sensors,^{2,7,11,16,17} and highly functionalized scaffolds for subsequent elaboration.^{3,4,6,10,12–15} We also reported that monolayers

of dendrimers containing Pt nanoparticles¹ having diameters in the 1–3 nm range act as electrocatalysts for oxygen reduction.¹⁸ This result implied that electrons were able to transfer from the electrode, through the dendrimer, and to the encapsulated metal. It also implied that O_2 was also able to move into the dendrimer interior and encounter the metal catalyst and that the product was able to move out of the dendrimer. Unfortunately, the monolayers used in these studies were not very efficient or stable because of their thinness and the weak interaction between the dendrimers and the electrode. Accordingly, we thought that it would be useful to prepare more resilient and thicker films having enhanced electrical conductivity.

To prepare such films we functionalized the periphery of PAMAM dendrimers with thiophene functional groups. We hypothesized that in the presence of 3-methylthiophene monomer (3MeTh) it would be possible to electrochemically copolymerize the dendrimers within a conducting P3MeTh matrix. There is precedence to support this hypothesis. For example, we^{3–5,10} and others^{19–22} have prepared composite dendrimer/polymer films by linking the dendrimer peripheral groups to

* To whom correspondence should be addressed. Tel: 979-845-5629. Fax: 979-845-1399. E-mail: crooks@tamu.edu.

(1) Crooks, R. M.; Zhao, M.; Sun, L.; Chechik, V.; Yeung, L. K. *Acc. Chem. Res.* **2001**, *34*, 181–190.

(2) Wells, M.; Crooks, R. M. *J. Am. Chem. Soc.* **1996**, *118*, 3988–3989.

(3) Zhou, Y.; Bruening, M. L.; Bergbreiter, D. E.; Crooks, R. M.; Wells, M. *J. Am. Chem. Soc.* **1996**, *118*, 3773–3774.

(4) Liu, Y.; Bruening, M. L.; Bergbreiter, D. E.; Crooks, R. M. *Angew. Chem., Int. Ed. Engl.* **1997**, *36*, 2114–2116.

(5) Liu, Y.; Zhao, M.; Bergbreiter, D. E.; Crooks, R. M. *J. Am. Chem. Soc.* **1997**, *119*, 8720–8721.

(6) Tokuhisa, H.; Zhao, M.; Baker, L. A.; Phan, V. T.; Dermody, D. L.; Garcia, M. E.; Pez, R. F.; Crooks, R. M.; Mayer, T. M. *J. Am. Chem. Soc.* **1998**, *120*, 4492–4501.

(7) Tokuhisa, H.; Crooks, R. M. *Langmuir* **1997**, *13*, 5608–5612.

(8) Zhao, M.; Tokuhisa, H.; Crooks, R. M. *Angew. Chem., Int. Ed. Engl.* **1997**, *36*, 2595–2598.

(9) Hierlemann, A.; Campbell, J. K.; Baker, L. A.; Crooks, R. M.; Ricco, A. J. *J. Am. Chem. Soc.* **1998**, *120*, 5323–5324.

(10) Zhao, M.; Liu, Y.; Crooks, R. M.; Bergbreiter, D. E. *J. Am. Chem. Soc.* **1999**, *121*, 923–930.

(11) Yoon, H. C.; Lee, D.; Kim, H. S. *Anal. Chim. Acta* **2002**, In press.

(12) Wang, J.; Chen, J.; Jia, X.; Cao, W.; Li, M. *Chem. Commun.* **2000**, 511–512.

(13) Tsukruk, V. V. *Adv. Mater.* **1998**, *10*, 253–257.

(14) Tsukruk, V. V.; Rinderspacher, F.; Bliznyuk, V. N. *Langmuir* **1997**, *13*, 2171–2176.

(15) Watanabe, S.; Regen, S. L. *J. Am. Chem. Soc.* **1994**, *116*, 8855–8856.

(16) Koo, B.; Song, C. K.; Kim, C. *Sens. Act. B* **2001**, *77*, 432–436.

(17) Losada, J.; Cuadrado, I.; Moran, M.; Casado, C. M.; Alonso, B.; Barranco, M. *Anal. Chim. Acta* **1997**, *338*, 191–198.

(18) Zhao, M.; Crooks, R. M. *Adv. Mater.* **1999**, *11*, 217–220.

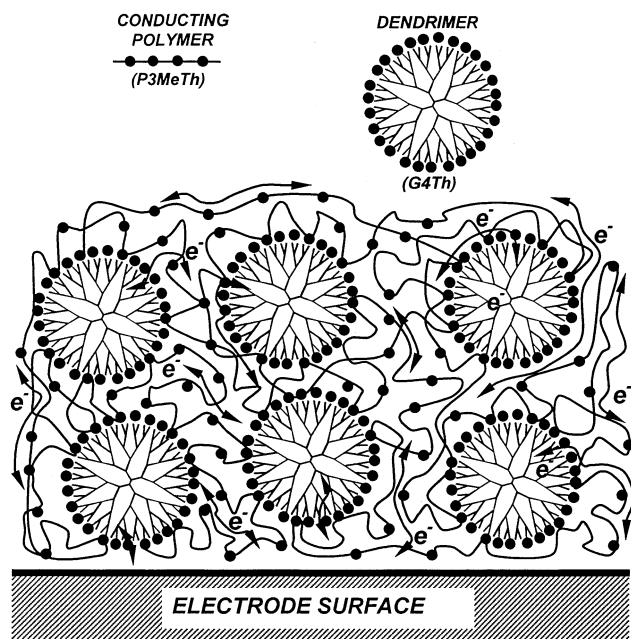
(19) Gröhn, F.; Kim, G.; Bauer, B. J.; Amis, E. J. *Macromolecules* **2001**, *34*, 2179–2185.

(20) Dvornic, P. R.; De Leuze-Jallouli, A. M.; Perz, S. V.; Owen, M. *J. Mol. Cryst. Liq. Cryst. Sci. Technol. A* **2000**, *353*, 223–236.

(21) Dvornic, P. R.; De Leuze-Jallouli, A. M.; Owen, M. J.; Perz, S. V. *Macromolecules* **2000**, *33*, 5366–5378.

(22) Sellner, H.; Karjalainen, J. K.; Seebach, D. *Chem. Eur. J.* **2001**, *7*, 2873–2887.

Scheme 1

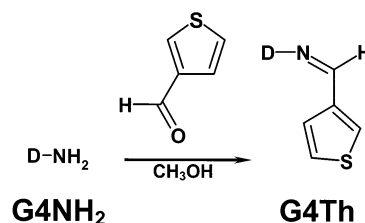


functional groups on a different type of polymer. For example, in one of our studies, we demonstrated that amine-terminated dendrimers form homogeneous composites with Gantrez, which is an active anhydride copolymer.^{4,5,10} These composite films exhibited fully reversible, pH-switchable permselectivity for both cationic and anionic redox-active probe molecules.⁵

There have been numerous reports concerning composite polymeric films rendered conductive by copolymerization with conductive polymers. For example, Heller^{23–26} and others^{27–29} have demonstrated the concept of “redox wiring” for electroactive enzymes embedded in surface-confined composites using conducting redox hydrogels²³ or polypyrrol chains functionalized with redox units such as ferrocene²⁷ and viologen.²⁹ Both the conductive polymer and the redox groups can act as redox mediators to carry electrons between the enzyme and the electrode surface. In the sense that dendrimers are somewhat akin to enzymes (similar chemical composition, size, and shape), our approach bears a clear relationship to these previous studies.

There have been a few reports describing electrically conductive dendrimer films. For example, Tomalia et al.^{30,31} have shown that PAMAM derivatives substituted with cationic naphthalene diimides can be arranged in π -stacks to yield conductive powders. Similarly, Fréchet et al.³² reported an example of a conductive poly-

Scheme 2



thiophene functionalized with dendritic side groups as solubilizers. The polymerizable groups were oligothiophenes tethered to the focal point of G2 and G3 aliphatic ether dendrimers. Conductivities as high as 200 S/cm were measured for iodine-doped thin films of these materials. Roncali and co-workers³³ reported the synthesis of electroactive conjugated polymers prepared by electropolymerization of increasing generations of phosphorus containing dendrimers derivatized with peripheral bithiophene groups.

The objective of our current work is to electrically wire together metal nanoparticles contained within dendrimers. In this first report we demonstrate that it is possible to electrochemically copolymerize 3MeTh with PAMAM dendrimers modified on their periphery with thiophene subunits. FTIR-external reflectance spectroscopy (FTIR-ERS) and electrochemical analysis of the resulting films indicate the presence of both the dendrimer and the thiophene monomer. In subsequent reports we will show that metal nanoparticles can be encapsulated within the dendrimer fraction of these conductive composite films.

Experimental Section

Reagents. Amine-terminated, fourth-generation PAMAM dendrimers (G4NH₂) were used as received from Dendritech, Inc. (Midland, MI). 3-Thiophenecarboxaldehyde and 3MeTh (Aldrich Chemical Co., Milwaukee, WI) were distilled before use. All solvents used were anhydrous grade or better. The supporting electrolytes N(C₄H₉)₄BF₄ and N(C₄H₉)₄PF₆ (Fluka) were electrochemical grade and used as received. NiSO₄ (Aldrich), CuSO₄·5H₂O (Fluka), and K₂PtCl₄ (Aldrich) were also used as received.

Synthesis of Thiophene-Functionalized PAMAM Dendrimers. Prior to use, methanol was removed by vacuum evaporation from G4NH₂ solutions to yield the solid material. Next, G4NH₂ was reacted with a 2-fold excess (128 equiv based on the 64 dendrimer terminal groups) of 3-thiophenecarboxaldehyde in dry methanol. The reaction was allowed to proceed for 3 days at room temperature under nitrogen. Excess aldehyde was removed by vacuum distillation until no aldehyde peak was detected by ¹H NMR. The resulting imine derivative was obtained in 98.5% yield and found to be soluble in methanol, chloroform, and dichloromethane. Scheme 2 shows the structures of the starting materials and the product of this reaction. MALDI and ESI mass spectrometry analyses failed to show the molecular ion peak at 20 231. However, ¹H NMR peak integration is consistent with full substitution of the terminal amines (Supporting Information, Figure S2). An uncertainty of about 5% in the integration could mean that the extent of substitution is as low as 95%. ¹H NMR (CD₃-OD): 8.27 (s, 64H, C₄H₃S), 7.81(s, 64H, C₄H₃S), 7.48(s, 64 H, C₄H₃S), 7.42 (s, 64H, N=CH), 3.62 (t, b, 128H, 64CH₂), 3.44(t, b, 128H, 64CH₂), 3.22 (t, b, 64H, 32CH₂), 3.16 (t, b, 64H, 32CH₂), 2.74 (t, b, 128H, 64CH₂), 2.67 (t, b, 128H, 64CH₂), 2.53

(23) Schmidtke, D. W.; Heller, A. *Anal. Chem.* **1998**, *70*, 2149–2155.

(24) Willner, I.; Heleg-Shabtai, V.; Blonder, R.; Katz, E.; Tao, G.; Buckmann, A. F.; Heller, A. *J. Am. Chem. Soc.* **1996**, *118*, 10321–10322.

(25) Rajagopalan, R.; Aoki, A.; Heller, A. *J. Phys. Chem.* **1996**, *100*, 3719–3727.

(26) Yarnitzky, C.; Caruana, A. M.; Schmidtke, D. W.; Heller, A. *J. Phys. Chem. B* **1998**, *102*, 10057–10061.

(27) Schuhmann, W. *Biosen., & Biolect.* **1995**, *10*, 181–193.

(28) Gun, J.; Lev, O. *Anal. Chim. Acta* **1996**, *336*, 95–106.

(29) Cosnier, S.; Galland, B.; Innocent, C. *J. Electroanal. Chem.* **1997**, *433*, 113–119.

(30) Miller, L. L.; Duan, R. G.; Tully, D. C.; Tomalia, D. A. *J. Am. Chem. Soc.* **1997**, *119*, 1005–1010.

(31) Duan, R. D.; Miller, L. L.; Tomalia, D. A. *J. Am. Chem. Soc.* **1995**, *117*, 10783–10784.

(32) Malenfant, P. R.; Fréchet, J. M. J. *Macromolecules* **2000**, *33*, 3634–3640.

(33) Sebastian, R. M.; Caminade, A. M.; Majoral, J. P.; Levillain, E.; Huchet, L.; Roncali, J. *Chem. Commun.* **2000**, 507–508.

(t, b, 64H, 32CH₂), 2.46 (t, b, 64H, 32CH₂), 2.31 to 2.26 (t, b, 228H, 114CH₂, overlapped). ¹³C {¹H} NMR (CD₃OD): (174.85) CONH, (159.94, 141.43, 131.68, 128.26, 126.82) N=CH-C₄H₃S, (61.17, 53.68, 51.32, 41.33, 38.81, 34.88) CH₂.

Electrochemistry. Working electrodes were Ti-primed Si(100) wafers sputter-coated with 200 nm of Au by Lance Goddard Associates (Foster City, CA). Before each experiment wafers were cleaned in a Model 135500 UV cleaner (Boekel Industries, Inc., Feasterville, PA) for 10 min. Afterward, the wafers were thoroughly rinsed with anhydrous ethanol and dried under flowing N₂. The approximate area of the Au substrates used for voltammetry and surface analysis was about 2.6 cm². In some experiments conventional Au disk (A ~ 0.020 cm²) working electrodes (Bioanalytical Systems, West Lafayette, IN) were used. The disk electrodes were polished for 5 min on a polishing cloth (Microcloth, Buehler, Lake Bluff, IL) using an aqueous 1 μm γ-Al₂O₃ (Buehler) slurry and then rinsed with deionized water. In all cases, the counter electrode was a Pt wire and the reference was Ag/AgCl (3 M NaCl) (Bioanalytical Systems, West Lafayette, IN).

Electrochemical experiments were carried out using a Princeton Applied Research (Princeton, NJ) Model 173 potentiostat and Model 175 Universal Programmer. The conductivity experiments were performed using a Pine Instruments AFRDE4 bipotentiostat (Grove City, PA) and Kipp and Zonen XYY' chart recorder (Bohemia, NY). Conductivity experiments were carried out using interdigitated gold array electrodes (15 μm lines and spaces) purchased from Microsensor Systems Inc. (Bowling Green, KY).

Spectroscopy. UV-vis reflectance spectroscopy was performed using a Hewlett-Packard 8453 UV-vis spectroscopy system equipped with a Lab Sphere (Wilmington, DE) Model RSA-HP8453 reflectance accessory. FTIR-ERS spectra were obtained using a FTS 6000 Spectrometer (Bio-Rad, Cambridge, MA) equipped with a Harrick Scientific (Ossining, NY) Seagull reflection accessory and a liquid N₂-cooled MCT detector. All spectra were the sum of 256 or fewer individual scans with *p*-polarized light at an 84° angle of incidence with respect to the Au substrate. In both UV-vis and FTIR-ERS a UV-cleaned Au substrate was used to acquire a background spectrum. X-ray photoelectron spectroscopic data (XPS) were acquired with an Axis HSi 165 Ultra Kratos instrument (Manchester, UK). XPS data acquisition employed a Al anode set at 15 mA and 15 KV. Ellipsometric thicknesses were determined using a Gaertner Scientific Model L2W26D ellipsometer (Chicago, IL), a wavelength of 633 nm, and an incident angle of 70°. A film refractive index (*n*) of 1.46 was assumed. On the basis of previous work from our group involving mono- and multilayers of PAMAM dendrimer, we believe the expected error for the thickness is about 4 Å.⁶ NMR characterization of the thiophene-derivatized dendrimer was carried out using a Varian VXR-300 spectrometer (Varian Associates, Palo Alto, CA) with the chemical shift reported in ppm referenced to TMS as an internal standard.

Results and Discussion

Characterization of Thin Films Prepared by Electrooxidation of Thiophene-Functionalized PAMAM Dendrimers. We began this study by examining the properties of the thiophene-terminated, fourth-generation PAMAM dendrimer (G4Th). Figure 1 shows the cyclic voltammetry of a CH₂Cl₂ solution containing 10 mM thiophene functional groups (Th) appended to G4Th (Th_{G4Th}) (i.e., the dendrimer concentration was 160 μM). An irreversible oxidation wave is present at an anodic peak potential (*E*_{p,a}) of 1.31 V, and a thin film formed on the surface of the electrode after several voltammetric scans. FTIR-ERS of this film revealed vibrations originating from the internal amide groups of the PAMAM dendrimers at 1659 and 1551 cm⁻¹ (Figure 2).^{6,34} The band centered at 1070 cm⁻¹ is

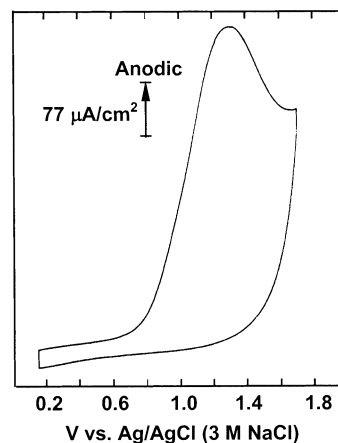


Figure 1. First growth scan (0.15–1.7 V) for a G4Th film prepared by electropolymerization of a solution containing 10 mM Th_{G4Th} ([G4Th] = 160 μM) and 0.1 M N(C₄H₉)₄BF₄ in CH₂Cl₂. A sputter-coated Au substrate (area ~ 2.6 cm²) was used as the working electrode. Scan rate, 100 mV/s.

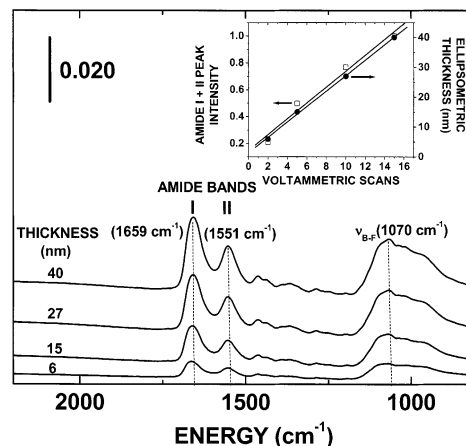


Figure 2. FTIR-ERS spectra of G4Th films of the indicated thicknesses. The films were prepared using a solution containing 1 mM Th_{G4Th} and 0.1 M N(C₄H₉)₄BF₄ in CH₂Cl₂. The number of growth scans was varied to control the film thickness. The inset indicates how the amide band intensity (amide I + amide II) and the ellipsometric thickness vary as a function of the number of voltammetric growth scans.

associated with the BF₄⁻ anion of the supporting electrolyte.³⁵

The inset in Figure 2 shows that the total integrated amide peak intensity (amide I + amide II, normalized to the largest absorption) increases linearly with the number of voltammetric scans. This trend in film thickness is confirmed by the ellipsometric measurements shown in the inset of Figure 2. During the course of 10 scans, the peak shape of the voltammogram shown in Figure 1 is gradually replaced with a potential-independent current that is characteristic of a purely capacitive response. This change, and also the initial absence of a reduction peak coupled to the oxidation wave, may be a consequence of limited polymer conjugation length, imposed by the dendrimer structure,

(34) Lin-Vien, D.; Colthup, N. B.; Fateley, W. G.; Grasselli, J. G. *The Handbook of Infrared and Raman Characteristic Frequencies of Organic Molecules*; Academic Press: San Diego, 1991.

(35) Nakamoto, K. *Infrared and Raman Spectra of Inorganic and Coordination Compounds Part A: Theory and Applications in Inorganic Chemistry*; John Wiley & Sons, Inc., 5th Ed.: New York, 1997.

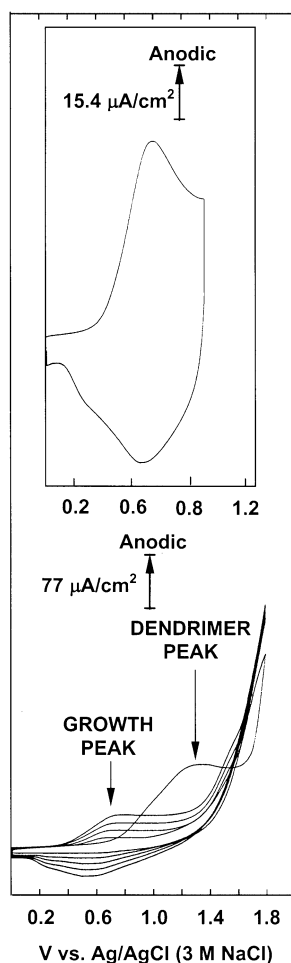


Figure 3. (Bottom) Voltammetric response for the electrocopolymerization of 3MeTh and G4Th prepared using a solution containing 1 mM Th_{G4Th} , 200 mM 3MeTh, and 0.1 M $\text{N}(\text{C}_4\text{H}_9)_4\text{BF}_4$ in CH_2Cl_2 . A sputter-coated Au surface was used as the working electrode (area $\sim 2.6 \text{ cm}^2$). Scan rate 100 mV/s (five scans). (Top) Voltammetry of the resulting P3MeTh/G4Th film in supporting electrolyte only (no monomer present).

coupled with overoxidation of the film during polymerization.³⁶ The maximum thickness of films such as these was about 100 nm, which is insufficient for obtaining conductivity data to test these ideas.

To improve the conductivity of the G4Th films, we thought it would be possible to copolymerize G4Th with the 3MeTh monomer. A similar approach has previously been used to connect electrochemically active enzymes to electrode surfaces.^{27,29} The copolymerization was carried out at a sputter-coated Au electrode ($\sim 2.6 \text{ cm}^2$) in a CH_2Cl_2 electrolyte solution containing 1 mM Th_{G4Th} and 200 mM 3MeTh. The bottom of Figure 3 shows the voltammetry resulting from five consecutive scans between 0.0 and 1.8 V in this solution. A peak associated with the irreversible electrooxidation of G4Th is apparent at 1.33 V, and a shoulder corresponding to oxidation of 3MeTh is present at 1.70 V. The anodic and cathodic peak potentials present at $E_{\text{p,a}} = 0.76 \text{ V}$ and $E_{\text{p,c}} = 0.53 \text{ V}$ result from reversible oxidation and reduction, respectively, of the composite copolymer. The voltammogram shown in the inset was obtained in a monomer-free electrolyte solution. A single, broad peak with $E_{\text{p,a}}$

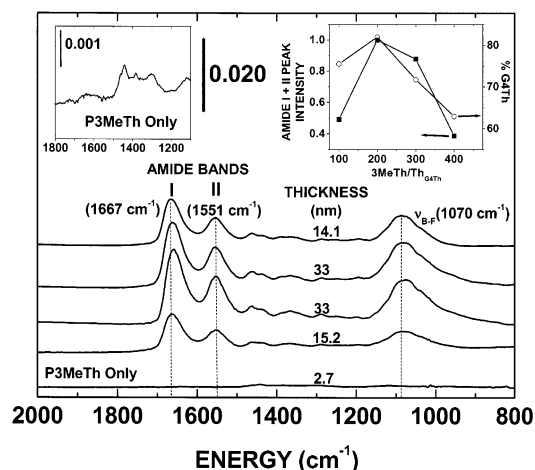


Figure 4. FTIR-ERS spectra of a copolymerized P3MeTh/G4Th film prepared using a solution containing 1 mM Th_{G4Th} and 0.1 M $\text{N}(\text{C}_4\text{H}_9)_4\text{BF}_4$ in CH_2Cl_2 and different concentrations of 3MeTh (from top to bottom: 400, 300, 200, 100 mM). The spectrum at the bottom corresponds to a P3MeTh film prepared in the absence of G4Th (expanded in the upper-right inset). The inset in the upper-right corner shows the total intensity of both amide bands (I + II) and the percentage of G4Th incorporated into the composite films for different ratios of 3MeTh/ Th_{G4Th} .

$= 0.67 \text{ V}$ and $E_{\text{p,c}} = 0.63 \text{ V}$ is observed. After 20 consecutive scans under these conditions, the peak anodic current ($i_{\text{p,a}}$) decreases by about 15%.

The dendrimer content of the films was optimized by polymerization of solutions containing different ratios of 3MeTh/ Th_{G4Th} . Figure 4 shows FTIR-ERS spectra for films prepared by scanning five times between 0.0 and 1.8 V in CH_2Cl_2 electrolyte solutions containing 1 mM Th_{G4Th} and different concentrations of the 3MeTh monomer. The amide I and II bands originating from the dendrimers, which are present at 1667 and 1551 cm^{-1} , respectively, were used to estimate the relative dendrimer content of the films. As mentioned previously, the peak at 1070 cm^{-1} originates from the BF_4^- counterion incorporated into the film during electropolymerization. For direct comparison to the composite films, a spectrum of a P3MeTh-only film (no dendrimer incorporation) is shown at the bottom of Figure 4 and expanded in the inset in the upper left corner of the figure. In the absence of G4Th, the large amide peaks are missing, but ring vibrations arising from P3MeTh are apparent at 1454, 1394, 1370, and 1168 cm^{-1} .³⁷ The inset in Figure 4 (upper right) shows the normalized amide intensity peak for different ratios of 3MeTh/ Th_{G4Th} prepared under the same experimental conditions. The amide intensity reaches a maximum when 3MeTh/ $\text{Th}_{\text{G4Th}} = 200$, indicating the highest level of dendrimer incorporation.

To estimate the percentage content of G4Th in the composite film, we compared the thickness and dendrimer content (based on the integration of the amide bands in the IR spectra) of both G4Th and P3MeTh/G4Th films. The slope of a plot of peak area vs thickness can be calculated for the G4Th film from a least-squares fit of the data in Figure 2; the numerical value is 0.050 nm^{-1} (correlation factor of 0.992). Using this value we

(36) Krische, B.; Zagorska, M. *Synth. Met.* **1989**, *28*, 263–268.

(37) Nalwa, H. S. *Handbook of Organic Conductive Molecules and Polymers*; John Wiley & Sons: New York, 1997; Vol. 2.

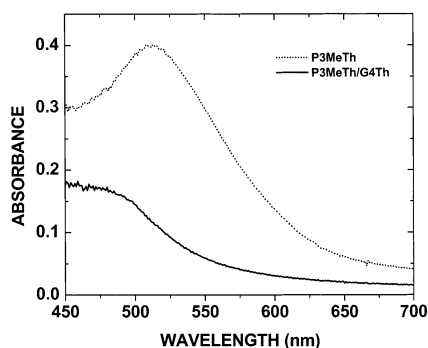


Figure 5. Visible reflectance spectra of P3MeTh and an electrocopolymerized P3MeTh/G4Th film prepared using the conditions described for Figure 3. The P3MeTh film was prepared using many growth cycles so that it would be thick enough to yield a spectrum.

calculated the theoretical amide intensity (I_{calc}) expected for a P3MeTh/G4Th film of known thickness. The experimental value of the amide intensity (I_{exp}) for the composite film was then used to estimate the percentage of G4Th in the composite film according to $(I_{\text{exp}}/I_{\text{calc}}) \times 100$. Since this calculation is based on intensity values for the amide bands by FTIR-ERS, the percentage is directly related to the number of dendrimer units within the films; however, the accuracy of this estimate relies on two assumptions. First, the amide intensity is linearly related to the thickness, as confirmed by the data in Figure 2. Second, the volume of the dendrimers in both the G4Th and P3MeTh/G4Th films is the same. The percentage of G4Th calculated for the composite films is shown in Figure 4 (inset upper right) and the values range from 60% to 80% G4Th.

Figure 5 shows visible reflectance spectra of both the P3MeTh and P3MeTh/G4Th composite films. The P3MeTh film exhibits a characteristic peak at about 510 nm,³⁸ but this peak is replaced by a blue-shifted shoulder centered at about 475 nm for the composite. This spectral change may arise from a change in the morphology of the copolymerized film that alters (probably reduces) the conjugation of the polythiophene chains.

Both the P3MeTh and P3MeTh/G4Th films displayed voltammograms characteristic of conductive films in pure supporting electrolyte solution (Figure 3).³⁸ In situ conductivity measurements obtained using an interdigitated array of electrodes³⁹ indicate that both P3MeTh and P3MeTh/G4Th films have a conductivity of 0.6 S/cm (Supporting Information, Figure S2). This value agrees well with the literature value of 1 S/cm for P3MeTh having PF_6^- as the counterion.³⁸ It may seem somewhat surprising that although the conductivity of both the composite and the P3MeTh-only films is the same, there is a blue shift in the peak present in the reflectance spectrum shown in Figure 5. Of course, the position of this peak is correlated to conjugation length and thus to conductivity. However, it has been known for many years that conductivity becomes independent of the length of individual thiophene oligomers after a relatively small number of repeat units, at which time

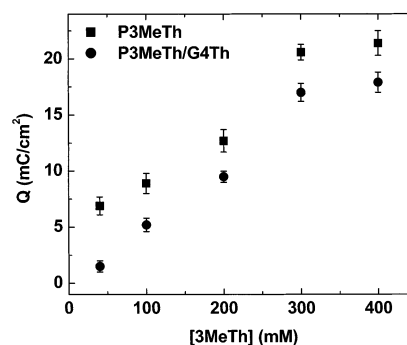


Figure 6. Total charge associated with both the anodic and cathodic peaks of thiophene-based films recorded during electrochemical cycling in supporting electrolyte solution $[0.1 \text{ M N}(\text{C}_4\text{H}_9)_4\text{BF}_4/\text{CH}_2\text{Cl}_2]$. Both P3MeTh/G4Th (circles) and P3MeTh (squares) films were prepared using different concentration of 3MeTh (40–400 mM). For the P3MeTh/G4Th films 1 mM Th_{G4Th} was used. Films were prepared using five growth cycles between 0 and 1.8 V.

conductivity becomes a function of more complex lattice phenomena.⁴⁰ The spectroscopic data, however, remain a strong function of conjugation.

Figure 6 correlates the total charge under both the anodic and cathodic peaks of the P3MeTh and P3MeTh/G4Th films to the concentration of 3MeTh monomer (for the composite film, $[\text{Th}_{\text{G4Th}}] = 1 \text{ mM}$) used to prepare the films. For all the concentrations of 3MeTh studied, the total charge associated with the P3MeTh/G4Th film (circles) was lower than that of P3MeTh film (squares). However, the percentage decrease was less as the concentration of 3MeTh present during the copolymerization step increased. For instance, the P3MeTh/G4Th film obtained with 40 mM 3MeTh shows a decrease of 78% in total charge compared to the corresponding P3MeTh film. However, the charge associated with the P3MeTh/G4Th film prepared using 400 mM of 3MeTh was only 16% lower than the corresponding P3MeTh film. This is an obvious consequence of the fact that when higher concentrations of 3MeTh are used, the composites are more like the P3MeTh-only films.

To demonstrate that the peripheral thiophene groups on the dendrimer are important for incorporation of the dendrimer into the P3MeTh/G4Th composite film, we copolymerized 3MeTh with a dendrimer that had no thiophene terminal groups. Because of the low solubility of amine-terminated PAMAM dendrimers in CH_2Cl_2 , we selected a poly(propylene imine) dendrimer (PPI) functionalized on the periphery with a 15-carbon alkyl chain (PPIC15). Despite the slight difference between the G4Th and PPIC15 dendrimers, the control experiment is still useful for demonstrating that peripheral thiophene functionalization is required to obtain a significant level of dendrimer incorporation into the thin films. Using identical synthetic conditions we prepared and characterized three types of films: P3MeTh, P3MeTh/G4Th, and P3MeTh/PPIC15. The voltammetric response of all three films (Supporting Information, Figure S3) result in values of $E_{\text{p,a}}$ and $E_{\text{p,c}}$ that are close to those discussed earlier for P3MeTh/G4Th (Figure 3).

The FTIR-ERS spectra for P3MeTh, P3MeTh/PPIC15, and P3MeTh/G4Th are shown in Figure 7. A spectrum

(38) Skotheim, T. A., Ed. *Handbook of Conducting Polymers*; Marcel Dekker: New York, 1986; Vol. 1.

(39) White, H. S.; Kittlesen, G. P.; Wrighton, M. S. *J. Am. Chem. Soc.* **1984**, *106*, 5375–5377.

(40) Skotheim, T. A.; Elsenbaumer, R. L.; Reynolds, J. R. *Handbook of Conducting Polymers*; 2nd ed.; Marcel Dekker: New York, 1998.

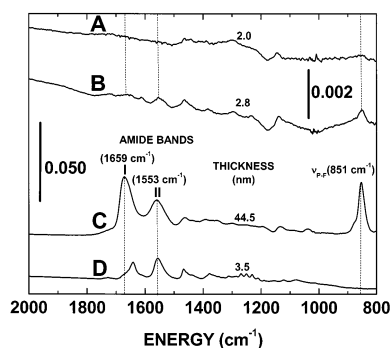


Figure 7. FTIR-ERS spectra for (A) P3MeTh, (B) P3MeTh/PPIC15, (C) P3MeTh/G4Th, and (D) chemisorbed PPIC15. The electrodeposited films A–C were prepared in 50 vol % $\text{CH}_2\text{Cl}_2/\text{CHCl}_3$ containing 200 mM 3MeTh, 0.1 M $\text{N}(\text{C}_4\text{H}_9)_4\text{PF}_6$, and 1 mM Th_{G4Th} or C15_{PPI}. The working electrode was sputtered Au (area $\sim 2.6 \text{ cm}^2$). The films were prepared by scanning between 0 and 1.8 V five times at 100 mV/s.

of a chemisorbed monolayer of PPIC15 is also included for reference (Figure 7D). The peak centered at 851 cm^{-1} is assigned to the counterion PF_6^- used for the preparation of the polymeric films.³⁵ The amide I and II bands for the chemisorbed PPIC15 monolayer appear at 1648 and 1553 cm^{-1} , respectively, indicating a slight red shift of the higher energy band with respect to the corresponding peak in the P3MeTh/G4Th composite film (1659 cm^{-1}). This is a consequence of the chemical environment of the amide bands, which is different in the two types of dendrimers. As discussed earlier, the P3MeTh film (Figure 7A) shows very low intensity peaks in the range $1500\text{--}1150 \text{ cm}^{-1}$, corresponding to ring vibrations. In contrast, the P3MeTh/PPIC15 film (Figure 7B) displays a series of low-intensity peaks in the amide region, indicating only slight incorporation of the PPI dendrimer. Comparison of the amide peak intensities in Figure 7, parts B and D, suggests that less than a single monolayer of PPIC15 is incorporated into the composite. Thickness values for these films corroborate this conclusion. The chemisorbed monolayer of PPIC15 dendrimer is about 3.5 nm thick, and the P3MeTh/PPIC15 and P3MeTh films are 2.8 and 2.0 nm thick, respectively. In contrast, the P3MeTh/G4Th composite film has a thickness of 44.5 nm, which is consistent with significant incorporation of dendrimer (65%). This is somewhat lower than the value shown in Figure 4 (82%) for the same composite film, but this is probably because two different solvents were used to prepare the films. Instead of pure CH_2Cl_2 , we used a mixture (50:50 v/v) of CH_2Cl_2 and CHCl_3 to accommodate the solubility of the PPIC15 dendrimer (Supporting Information, Figure S3). High-resolution XPS spectra confirmed the presence of a small amount of nitrogen in the composite P3MeTh/PPIC15 film (Supporting Information, Figure S4).

Absorption of Transition Metal Ions into the Composite Dendrimer Films. A primary objective of this research is the incorporation of dendrimer-encapsulated nanoparticles^{1,18,41} into these composite films. As a first step toward that goal we compared the uptake of Cu^{2+} , Ni^{2+} , and Pt^{2+} into P3MeTh and P3MeTh/G4Th thin films in an effort to detect differences resulting

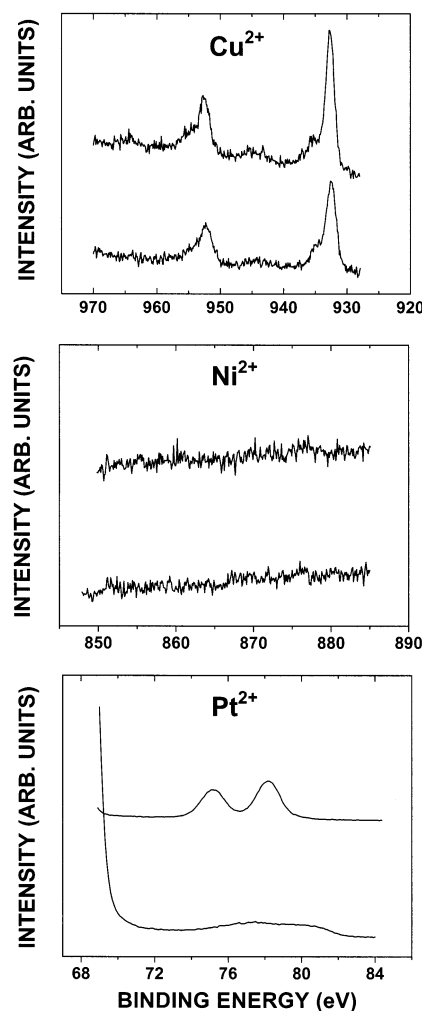


Figure 8. High-resolution XPS spectra for P3MeTh (bottom) and P3MeTh/G4Th (top) films (prepared as in Figure 3) after exposure to 10 mM aqueous solutions of Cu^{2+} , Ni^{2+} , and Pt^{2+} .

from the presence of the metal-ion-complexing dendrimers. Separate P3MeTh and P3MeTh/G4Th films on Au substrates were exposed to aqueous 10 mM solutions of each of the three metal ions. After rinsing with water and carefully drying under flowing nitrogen, the films were analyzed by XPS. Figure 8 displays the high-resolution spectra recorded for both P3MeTh (bottom spectrum) and P3MeTh/G4Th (top spectrum) after exposure to the three metal-ion solutions. The results indicate that both films incorporate Cu^{2+} , as indicated by the presence of $2p_{1/2}$ and $2p_{3/2}$ photoelectron peaks at 953 and 933 eV, respectively. Similarly, neither P3MeTh/G4Th nor P3MeTh have an affinity for Ni^{2+} , as confirmed by the absence of lines in the Ni 2p region ($2p_{1/2}$, 870 eV; $2p_{3/2}$, 853 eV). In contrast, Pt^{2+} has a clear affinity for the dendrimer-containing polymer thin film. Specifically, the $4f_{5/2}$ (79.2 eV) and $4f_{7/2}$ (76 eV) lines for Pt^{2+} are only present in the P3MeTh/G4Th spectrum (top), implying selective affinity for Pt^{2+} ions compared to the P3MeTh control (bottom). Films prepared by electrodeposition of G4Th without using 3MeTh as a copolymer were also found to absorb Pt^{2+} , corroborating the affinity of Pt^{2+} for the surface-confined dendrimers. This finding is consistent with previously reported results for amine-containing dendrimers in solution and in other polymers.^{1,2,18,19,41}

(41) Zhao, M.; Sun, L.; Crooks, R. M. *J. Am. Chem. Soc.* **1998**, *120*, 4877–4878.

Summary and Conclusions

In summary, we have reported the electrochemical preparation of conductive films incorporating significant amounts of PAMAM dendrimers by copolymerization of poly(3-methylthiophene) and a thiophene-terminated PAMAM dendrimer. Control experiments confirm that the peripheral thiophene groups are required for dendrimer incorporation into the film. We suspect this is a consequence of covalent bond formation between the dendrimers and the growing P3MeTh chains. The conductivities of the P3MeTh films with and without incorporation of the dendrimer are similar in magnitude. Importantly, we have also shown that dendrimers incorporated into P3MeTh thin films display an affinity for Pt^{2+} that is not observed for the P3MeTh-only film. We believe, but have not yet conclusively shown, that these ions are encapsulated within the dendrimers. The significant result of this work, then, is that these conductive composite films may provide a means for

wiring together dendrimer-encapsulated metal nanoparticles. We shall report further on this objective soon.

Acknowledgment. We gratefully acknowledge the Office of Naval Research for full financial support of this work. We thank the Materials Characterization Facility of the TAMU Center for Integrated Microchemical Systems for access to the Kratos XPS.

Supporting Information Available: Figure S1, ^1H NMR spectrum of G4Th showing the integration ratios to confirm full substitution of the PAMAM dendrimer; Figure S2, conductivity as a function of potential for P3MeTh and P3MeTh/G4Th; Figure S3, voltammograms for P3MeTh, P3MeTh/G4Th, and P3MeTh/PPIC15 films prepared by electropolymerization in 50 vol % CH_2Cl_2 and CHCl_3 ; and Figure S4, XPS spectra of P3MeTh and P3MeTh/PPIC15 films prepared by electropolymerization in 50 vol % CH_2Cl_2 and CHCl_3 . This material is available free of charge via the Internet at <http://pubs.acs.org>.

CM020635S